Upwind Parabolized Navier-Stokes Code for Chemically Reacting Flows

John C. Tannehill,* John O. Ievalts,† and Philip E. Buelow†
Engineering Analysis, Inc., Ames, Iowa
Dinesh K. Prabhu†
Eloret Institute, Sunnyvale, California
and
Scott L. Lawrence†
NASA Ames Research Center, Moffett Field, California

A new upwind, parabolized Navier-Stokes (PNS) code has been developed to compute the hypersonic, viscous, chemically reacting flow around two-dimensional or axisymmetric bodies. The new code is an extension of the upwind (perfect gas) PNS code of Lawrence, Tannehill, and Chaussee. The upwind algorithm is based on Roe's flux-difference splitting scheme, which has been modified to account for real gas effects. The algorithm solves the gasdynamic and species continuity equations in a loosely coupled manner. The new code has been validated by computing the $M_\infty = 25$ laminar flow of chemically reacting air over a wedge and a cone. The results of these computations are compared with the results from a centrally differenced, fully coupled, nonequilibrium PNS code. The agreement is excellent, except in the vicinity of the shock wave, where the present code exhibits superior shock-capturing capabilities.

Introduction

THE renewed interest in hypersonic aerothermodynamics has led to the development of several new parabolized Navier-Stokes (PNS) codes that account for real gas effects. These codes have been written for either equilibrium[1-7] or nonequilibrium[8-14] chemistry and have been applied to both two- and three-dimensional geometries. Most of these codes are based on centrally differenced algorithms such as the Beam-Warming scheme.[15] One of the major drawbacks of this type of algorithm is that the central differencing of fluxes across flowfield discontinuities tends to introduce errors into the solution in the form of local flow property oscillations. In order to control these oscillations, some type of artificial dissipation is required. The correct magnitude of this added "smoothing" is generally left for the user to specify through some sort of trial-and-error process.

To overcome this difficulty, Lawrence et al.[16,17] have developed an upwind PNS code that is based on Roe's approximate Riemann solver.[18] The dissipation term associated with this scheme is sufficiently adaptive to flow conditions so that, even when attempting to capture very strong shock waves, no additional smoothing is required. The superior shock-capturing capability of this upwind PNS code has been demonstrated for both two-dimensional[16] and three-dimensional[17] perfect gas flows. Recently, this code was extended by the present authors[19] to permit equilibrium air computations. The upwind algorithm was modified to account for real gas effects.

Presented as Paper 88-2614 at the AIAA Thermophysics, Plasmadynamics, and Lasers Conference, San Antonio, Texas, June 27-29, 1988; received July 28, 1988.

*President; currently Manager, Computational Fluid Dynamics Center, and Professor, Department of Aerospace Engineering, Iowa State University, Ames, IA. Associate Fellow AIAA.
†Research Scientist. Member AIAA.

In the present work, the upwind PNS code of Lawrence et al.[16] has been further extended to permit computations of chemically reacting flowfields. The gasdynamic equations and the species continuity equations are solved in a loosely coupled manner using a procedure similar to the one employed by Balakrishnan[20] for the thin-layer Navier-Stokes equations. The advantage of using this approach for the present upwind code is that the general form of the gasdynamic equations remains the same for both equilibrium and nonequilibrium calculations, with the exception of the diffusion term in the energy equation. Since the chemistry effects are introduced into the gasdynamic equations through an "effective gamma," it is possible to modify Roe's scheme for nonequilibrium calculations in the same manner as for equilibrium calculations. Thus, a single code can be readily developed that permits either perfect gas, equilbrium air, or nonequilibrium calculations to be performed. This was the approach taken in the present study. The resulting two-dimensional/axisymmetric code has been used to compute the $M_\infty = 25$ laminar flow of chemically reacting air over a 10-deg half-angle wedge and cone. The results of these computations are compared with those obtained using the centrally differenced, fully coupled, nonequilibrium, PNS code of Prabhu et al.[10]

Governing Equations

Gasdynamic Equations

The PNS equations are obtained from the compressible Navier-Stokes equations by dropping the unsteady terms and neglecting the streamwise viscous derivatives in comparison with the normal viscous derivatives. The resulting equations, which are expressed in (ξ,η) computational coordinates via the transformation $\xi = x$ and $\eta = \eta(x,y)$, can be written in nondimensional form for a two-dimensional ($\delta = 0$) or axisymmetric ($\delta = 1$) nonreacting flow as

$$\frac{\partial E}{\partial \xi} + \frac{\partial F}{\partial \eta} + G = 0 \tag{1}$$

where

$$E = E_i/J$$

$$F = \left[\eta_x(E_i - E_v) + \eta_y(F_i - F_v)\right]/J$$

$$G = \delta(G_i - G_v)/J$$

and

$$E_i = [\rho u,\ \rho u^2 + p,\ \rho uv,\ \rho u h_t]^T$$

$$F_i = [\rho v,\ \rho uv,\ \rho v^2 + p,\ \rho v h_t]^T$$

$$G_i = \frac{1}{y}[\rho v,\ \rho uv,\ \rho v^2,\ \rho v h_t]^T$$

$$E_v = \frac{\mu}{Re_\infty}\left[0,\ \frac{4}{3}\eta_x u_\eta - \frac{2}{3}\eta_y v_\eta,\ \eta_y u_\eta + \eta_x v_\eta,\ u\left(\frac{4}{3}\eta_x u_\eta - \frac{2}{3}\eta_y v_\eta\right) + v\left(\eta_y u_\eta + \eta_x v_\eta\right) + \eta_x \frac{k}{\mu} T_\eta / \left[(\gamma_\infty - 1)M_\infty^2 Pr_\infty\right]\right]^T$$

$$F_v = \frac{\mu}{Re_\infty}\left[0,\ \eta_y u_\eta + \eta_x v_\eta,\ -\frac{2}{3}\eta_x u_\eta + \frac{4}{3}\eta_y v_\eta,\ u\left(\eta_y u_\eta + \eta_x v_\eta\right) + v\left(-\frac{2}{3}\eta_x u_\eta + \frac{4}{3}\eta_y v_\eta\right) + \eta_y \frac{k}{\mu} T_\eta / \left[(\gamma_\infty - 1)M_\infty^2 Pr_\infty\right]\right]^T$$

$$G_v = \frac{1}{yRe_\infty}\left[0,\ -\frac{2}{3}y\eta_x(\mu v/y)_\eta + \mu(\eta_x v_\eta + \eta_y u_\eta) - \frac{2}{3}y\eta_y(\mu v/y)_\eta + 2\mu(\eta_y v_\eta - v/y) - \frac{2}{3}y\eta_x(\mu uv/y)_\eta - \frac{2}{3}\eta_y(\mu v^2)_\eta + \frac{1}{2}\mu\eta_y(u^2 + v^2)_\eta + \mu(u\eta_x v_\eta + v\eta_y u_\eta) - \frac{2}{3}\mu v(\eta_x u_\eta + \eta_y v_\eta)_\eta - \eta_y k T_\eta / \left[(\gamma_\infty - 1)M_\infty^2 Pr_\infty\right]\right]^T$$

$$e_t = \rho\left[e + (u^2 + v^2)/2\right]$$

$$h_t = (e_t + p)/\rho$$

In these equations, p is the nondimensional pressure; ρ the density; T the temperature; u the velocity component in the x direction; v the velocity component in the y direction; e the internal energy; μ the coefficient of viscosity; k the coefficient of thermal conductivity; M_∞ the freestream Mach number; Re_∞ the Reynolds number; Pr_∞ the Prandtl number; γ_∞ the ratio of specific heats; and J the Jacobian of the transformation ($J = \eta y$). The equations have been nondimensionalized (dimensional quantities are denoted by a tilde) in the following manner:

$$\xi = \tilde{\xi}/\tilde{L} \qquad \eta = \tilde{\eta}/\tilde{L} \qquad u = \tilde{u}/\tilde{V}_\infty \qquad v = \tilde{v}/\tilde{V}_\infty$$

$$p = \tilde{p}/\tilde{\rho}_\infty \tilde{V}_\infty^2 \qquad \rho = \tilde{\rho}/\tilde{\rho}_\infty \qquad T = \tilde{T}/\tilde{T}_\infty \qquad e = \tilde{e}/\tilde{V}_\infty^2$$

$$\mu = \tilde{\mu}/\tilde{\mu}_\infty \qquad k = \tilde{k}/\tilde{k}_\infty \qquad Re_\infty = \tilde{\rho}_\infty \tilde{V}_\infty \tilde{L}/\tilde{\mu}_\infty \tag{2}$$

where $\tilde{L}$ is the reference length of unity, and $\tilde{V}_\infty$ is the freestream velocity.

In order to "close" the preceding system of PNS equations, relations between the thermodynamic variables are required along with expressions for the transport properties $\tilde{\mu}$ and $\tilde{k}$. The pressure is computed from the relation

$$\tilde{p} = (\bar{\gamma} - 1)\tilde{\rho}\tilde{e} \tag{3}$$

where $\bar{\gamma}$ is defined by

$$\bar{\gamma} = \tilde{h}/\tilde{e} \tag{4}$$

For perfect gas computations, $\bar{\gamma} = \gamma_\infty$. For equilibrium air computations, $\bar{\gamma}$ and all other thermodynamic and transport properties are obtained from the simplified curve fits of Srinivasan et al.[21,22] For nonequilibrium computations, the thermodynamic and transport properties are determined using the equations given in the next section.

The PNS equations are a mixed set of hyperbolic-parabolic equations in the streamwise direction ξ, provided that the inviscid flow is supersonic, the streamwise velocity component is greater than zero everywhere, and the streamwise pressure gradient term in the streamwise momentum equation is either omitted in subsonic regions or the "departure behavior" is suppressed by a suitable technique. In the present study, the technique of Vigneron et al.[23] is used to prevent departure solutions. The Vigneron technique involves splitting the E vector into two parts:

$$E = E^* + P \tag{5}$$

where

$$E^* = \frac{1}{J}[\rho u,\ \rho u^2 + \omega p,\ \rho uv,\ \rho u h_t]^T$$

$$P = \frac{1}{J}\left[0,\ (1-\omega)p,\ 0,\ 0\right]^T$$

The E^* vector now replaces E in the numerical scheme, and P is treated as a source term that is either neglected or evaluated in the supersonic region. The final form of the governing equations becomes

$$\frac{\partial E^*}{\partial \xi} + \frac{\partial F}{\partial \eta} + \frac{\partial P}{\partial \xi} + G = 0 \tag{6}$$

If P is neglected in the subsonic viscous region, an eigenvalue analysis for real gas flows[10] shows that the PNS equations are hyperbolic-parabolic in the ξ direction, provided that

$$\omega = \begin{cases} \dfrac{\bar{\gamma}M_\xi^2}{1 + (\bar{\gamma} - 1)M_\xi^2}, & M_\xi < 1 \\ 1, & M_\xi \geq 1 \end{cases} \tag{7}$$

where M_ξ is the local streamwise Mach number.

Equations for Nonequilbrium Flow

For nonequilibrium flows, the species continuity equations must be solved in addition to the gasdynamic equations given previously. The gasdynamic equations remain the same except for the additional term in the energy equation, which is due to the diffusion of the species. The nondimensional species continuity equations, expressed in transformed coordinates, are given by

$$\frac{\partial c_s}{\partial \xi} + \left(\eta_x + \frac{v}{u}\eta_y\right)\frac{\partial c_s}{\partial \eta} = \frac{1}{\rho u}\left[\dot{\omega}_s + \frac{\eta_y}{Re_\infty}\frac{\partial}{\partial \eta}\left(\beta_3 \rho D \eta_y \frac{\partial c_s}{\partial \eta}\right) + \frac{\eta_x}{Re_\infty}\frac{\partial}{\partial \eta}\left(\beta_3 \rho D \eta_x \frac{\partial c_s}{\partial \eta}\right) + \frac{\delta}{y}\frac{\eta_y}{Re_\infty}\left(\beta_3 \rho D \frac{\partial c_s}{\partial \eta}\right)\right], \qquad s = 1,2,\ldots,n \tag{8}$$

where c_s is the mass fraction of species s, $\dot{\omega}_s$ is the nondimensional production term, D is the nondimensional binary diffusion coefficient, and $\beta_3 = \tilde{\rho}_\infty \tilde{D}_\infty/\tilde{\mu}_\infty$.

The chemical model used in the present calculations is identical to the air model employed by Prabhu et al.[10] It consists of molecular oxygen (O_2), atomic oxygen (O), molecular nitrogen (N_2), atomic nitrogen (N), and nitric oxide (NO). The species are indexed $s = 1,2,\ldots,5$ in this order. The following reactions are considered between the constituent species:

$$\begin{aligned}
&(1)\ O_2 + M_1 \rightleftarrows 2O + M_1\\
&(2)\ N_2 + M_2 \rightleftarrows 2N + M_2\\
&(3)\ N_2 + N \rightleftarrows 2N + N\\
&(4)\ NO + M_3 \rightleftarrows N + O + M_3\\
&(5)\ NO + O \rightleftarrows O_2 + N\\
&(6)\ N_2 + O \rightleftarrows NO + N
\end{aligned} \tag{9}$$

where M_1, M_2, and M_3 are catalytic third bodies. The preceding model has five species ($n = 5$), six reactions ($m = 6$), and eight reactants ($n_t = 8$). These reactions can be represented symbolically as

$$\sum_{l=1}^{n_t} \nu'_{k,l} A_l \rightleftharpoons \sum_{l=1}^{n_t} \nu''_{k,l} A_l, \qquad k = 1,2,\ldots,m \tag{10}$$

where $\nu'_{k,l}$ and $\nu''_{k,l}$ are the stoichiometric coefficients, and A_l is the chemical symbol of the lth species. Using the law of mass action, the nondimensional mass production rate of species s is

$$\dot{\omega}_s = \mathfrak{M}_s \sum_{k=1}^{m} (\nu''_{k,s} - \nu'_{k,s}) \left\{ K_{f,k}(T) \prod_{r=1}^{n_t} [\rho\gamma_r]^{\nu'_{k,r}} - K_{b,k}(T) \prod_{r=1}^{n_t} [\rho\gamma_r]^{\nu''_{k,r}} \right\} \tag{11}$$

where γ_r is the nondimensional mole-mass ratio of the reactants, and $\mathfrak{M}_s$ is the molecular weight of species s. Further details on the reaction rates are given in Ref. 24.

The enthalpies and specific heats of the species are obtained from the following relations:

$$\begin{aligned}
\tilde{h}_s &= \tilde{T} \cdot C_{1,s}(\tilde{T}) + \tilde{h}_s^0\\
\tilde{C}_{p,s} &= C_{2,s}(\tilde{T})
\end{aligned} \tag{12}$$

Tables of $C_{1,s}$ and $C_{2,s}$ as a function of $\tilde{T}(K)$ are obtained from Ref. 25. Cubic spline interpolation is used in these tables. The enthalpy and frozen specific heat of the mixture are given by the following expressions:

$$\begin{aligned}
\tilde{h} &= \sum_{s=1}^{n} c_s \tilde{h}_s\\
\tilde{C}_{p_f} &= \left.\frac{\mathrm{d}\tilde{h}}{\mathrm{d}\tilde{T}}\right|_{c_1,\ldots,c_n} = \sum_{s=1}^{n} c_s \frac{\mathrm{d}\tilde{h}_s}{\mathrm{d}\tilde{T}} = \sum_{s=1}^{n} c_s \tilde{C}_{p,s}
\end{aligned} \tag{13}$$

where the subscripts on the differentiation indicate that the composition of the mixture is frozen locally.

The viscosity of species s is calculated from curve fits developed in Ref. 25, and the thermal conductivity is computed using Eucken's semiempirical formula. The viscosity and thermal conductivity of the mixture are determined using Wilke's semiempirical mixing rule.[26]

The binary Lewis numbers for all the species are assumed to be the same constant Le. The kinematic binary diffusion coefficient D is then computed from the definition

$$D = \frac{\tilde{\kappa} Le}{\tilde{\rho} \tilde{C}_{p_f} \tilde{D}_\infty} \tag{14}$$

Finally, the equation of state for a mixture of perfect gases is given by

$$p = \frac{\beta_1 \rho T}{\mathfrak{M}} \tag{15}$$

where

$$\mathfrak{M} = \left(\sum_{s=1}^{n} \frac{c_s}{\mathfrak{M}_s} \right)^{-1}, \qquad \beta_1 = \frac{\tilde{R}\tilde{T}_\infty}{\tilde{\mathfrak{M}}_\infty \tilde{V}_\infty^2}$$

Numerical Method

Numerical Solution of Gasdynamic Equations

The algorithm used in the present real gas code to solve the gasdynamic equations is a modified version of the upwind, finite-volume algorithm developed by Lawrence et al.[16] to solve the (perfect gas) PNS equations. The upwind algorithm is based on Roe's scheme,[18] which has been adapted for real gas space-marching calculations using a similar procedure to the one applied by Grossman and Walters[27] to an upwind, time-dependent Euler code. Their procedure, which relies on the previous work of Colella and Glaz,[28] has been adapted in the current study to the steady PNS equations. The present procedure for solving the gasdynamic equations is described in detail in Ref. 19.

Numerical Solution of Species Continuity Equations

For chemical nonequilibrium computations, the species continuity equations must be integrated along with the gasdynamic equations. This can be accomplished in a variety of ways, including the fully coupled approach and the loosely coupled approach. In the fully coupled approach, the gasdynamic equations and the species continuity equations are solved simultaneously using the same implicit algorithm. The advantage of this approach is that, for flows near equilibrium, the marching step size is not severely restricted. The disadvantage is that, as the number of species increases, the size of the block matrices that need to be inverted increases in a corresponding fashion. Thus, the calculations may require a substantial amount of computer time.

In the loosely coupled approach, the gasdynamic equations and the species continuity equations are solved separately. The coupling between the two sets of equations is then obtained in an approximate manner. In the approach of Balakrishnan,[20] the coupling between the gasdynamics and the chemistry is primarily achieved through $\bar{\gamma}$, which appears in the equation of state given by Eq. (3). The solution of the gasdynamic equations yields the velocity, density, and pressure fields. The species continuity equations are then integrated to obtain the mass fractions. With the mass fractions known and the pressure and enthalpy fixed, the molecular weight, temperature, density, and $\bar{\gamma}$ can be computed. The species continuity equations are then integrated again (using the updated temperature), and the previously mentioned procedure is repeated. As the final step, the density and total energy from the gasdynamic solution are corrected.

In the present study, the gasdynamic equations and the species continuity equations are solved in a manner similar to the loosely coupled approach of Balakrishnan. One of the differences between the present approach and the Balakrishnan approach is that density, instead of pressure, is held fixed during the chemistry iteration. The species continuity equations are

solved using the following implicit upwind scheme:

$$(c_s)_j^{n+1} = (c_s)_j^n - \lambda_j^{n+1}\frac{\Delta\xi}{\Delta\eta}\left[(c_s)_j^{n+1} - (c_s)_{j-1}^{n+1}\right] + \frac{\Delta\xi}{(\rho u)_j^n}$$
$$\times\Bigg((\dot{\omega}_s)_j^n + \frac{\beta_3}{(\Delta\eta)^2 Re_\infty}(\eta_y)_j^n\Big\{(\rho D\eta_y)_{j+\frac{1}{2}}^n\left[(c_s)_{j+1}^{n+1} - (c_s)_j^{n+1}\right]$$
$$-(\rho D\eta_y)_{j-\frac{1}{2}}^n\left[(c_s)_j^{n+1} - (c_s)_{j-1}^{n+1}\right]\Big\} + \frac{\beta_3}{(\Delta\eta)^2 Re_\infty}(\eta_x)_j^n$$
$$\times\Big\{(\rho D\eta_x)_{j+\frac{1}{2}}^n\left[(c_s)_{j+1}^{n+1} - (c_s)_j^{n+1}\right] - (\rho D\eta_x)_{j-\frac{1}{2}}^n$$
$$\times\left[(c_s)_j^{n+1} - (c_s)_{j-1}^{n+1}\right]\Big\} + \frac{\beta_3\delta}{2\Delta\eta Re_\infty}\left(\frac{\rho D\eta_y}{y}\right)_j^n$$
$$\times\left[(c_s)_{j+1}^{n+1} - (c_s)_{j-1}^{n+1}\right]\Bigg), \qquad s = 1,2,\ldots,n \tag{16}$$

where λ is given by

$$\lambda = \eta_x + (v/u)\eta_y$$

and is assumed positive for the backward-differenced algorithm given in Eq. (16). If λ is negative, a forward difference is employed for the convection term $\partial c_s/\partial\eta$. The convection term in this equation is modeled with a first-order-accurate upwind difference, and the diffusion terms are modeled by second-order-accurate central differences. It was found that modeling the convection term with a second-order-accurate upwind difference had little effect on the species mass fraction profiles computed in this study.

Once the mass fractions of the species are calculated from Eq. (16) and the enthalpy is determined from the solution of the gasdynamic equations at $n+1$, the temperature is obtained from Eq. (13) using the Newton-Raphson iteration method. The Newton-Raphson algorithm applied to this equation is

$$\tilde{T}^{k+1} = \tilde{T}^k - \frac{g(\tilde{T}^k) - \tilde{h}}{g'(\tilde{T}^k)} \tag{17}$$

where

$$g(\tilde{T}) = \sum_{s=1}^{n} c_s \tilde{h}_s(\tilde{T})$$
$$g'(\tilde{T}) = \sum_{s=1}^{n} c_s \tilde{C}_{p,s}(\tilde{T})$$

and k is the index of iteration. The iterations are continued until

$$|\tilde{T}^{k+1} - \tilde{T}^k| \le \epsilon$$

where ϵ is a small positive quantity. Once the temperature is determined, the pressure can be computed from Eq. (15) and $\bar{\gamma}$ can be obtained from Eq. (3). For cases where the species mass fractions are changing rapidly, the gasdynamic equations and the species continuity equations can be recomputed at the $n+1$ level in an iterative manner to enhance the coupling between the chemistry and the fluids. This was found to be unnecessary for the calculations performed in this study. Also, the effect of the diffusion heat flux term in the energy equation was negligible for the present calculations but has been found to be important at more severe conditions.

Numerical Results

The present upwind, chemical nonequilibrium, PNS code has been validated by computing the hypersonic laminar flow of dissociating air over a wedge and a cone. The present results are compared with those calculated by using the centrally differenced, nonequilibrium, PNS code developed by Prabhu et al.[10] It should be noted that the code of Prabhu et al. solves the gasdynamic and species conservation equations in a fully coupled manner rather than in the loosely coupled approach of the present method.

Test Case I

The first test case computed was that of hypersonic, laminar flow of chemically reacting air over a 10-deg half-angle wedge. The flow conditions for this test case correspond to an altitude of 60.96 km where the ambient pressure and temperature are 20.35 N/m^2 and 252.6 K, respectively. The other pertinent flow parameters are

$M_\infty = 25.3$ $\quad c_{1_\infty} = 0.21$ $\quad (O_2)$

$Re_\infty = 1.29\times10^5$ $\quad c_{3_\infty} = 0.79$ $\quad (N_2)$

$\tilde{V}_\infty = 8100$ m/s $\quad c_{2_\infty} = c_{4_\infty} = c_{5_\infty} = 0$

$\tilde{T}_w = 1200$ K $\quad Le = 1.4$

The coordinate system for this test case is shown in Fig. 1. The grid used for both codes consisted of 60 points in the η direction. The distance of the first point above the wedge surface was specified as 1.0×10^{-4} m, and this value was used to determine the appropriate Roberts stretching parameter[29] β for the remaining points. The ξ = const grid lines were placed normal to the x axis, and the height of the top boundary was kept fixed at 0.15 m from the body surface. The initial conditions for both codes (at $\tilde{x}=0$) were provided by specifying freestream conditions everywhere except at the wall, where no-slip conditions and constant wall temperature were imposed. The solution was then marched 2000 steps downstream with a 5×10^{-4} m step size and terminated at $\tilde{x}=1.0$ m.

The tangential velocity and temperature profiles at $\tilde{x}=1.0$ m are compared in Figs. 2 and 3, respectively. The tangential velocity is defined as

$$u_t = u\cos\theta + v\sin\theta \tag{18}$$

where θ is the wedge half-angle. The comparison is excellent except near the bow shock region, where the centrally differenced PNS code "smears" the solution over five or six mesh points, whereas the present upwind code resolves the discontinuity in typically three mesh points. The smearing of the centrally differenced solution is a result of the artificial smoothing necessary to maintain a monotonic profile in the shock region. The nonequilibrium temperature profile is compared in Fig. 4 with the equilibrium and perfect gas ($\gamma_\infty = 1.4$) temperature profiles. All of these profiles were computed with the present code. This code is written so that the user can specify whether a perfect gas, equilibrium air, or nonequilibrium calculation is to be performed by simply setting the input parameter *IGAS* equal to 0, +1, or −1, respectively. The O_2, O, N_2, N, and NO mass fractions at $\tilde{x}=1.0$ m are compared in Figs. 5 and 6. A

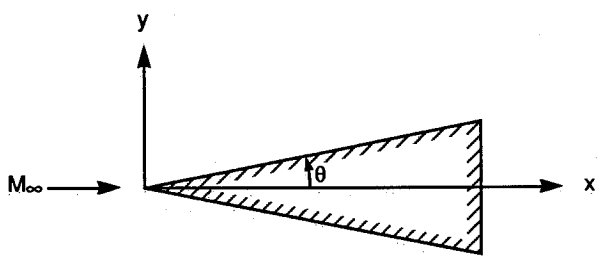

Fig. 1 Coordinate system for the wedge and cone test cases.

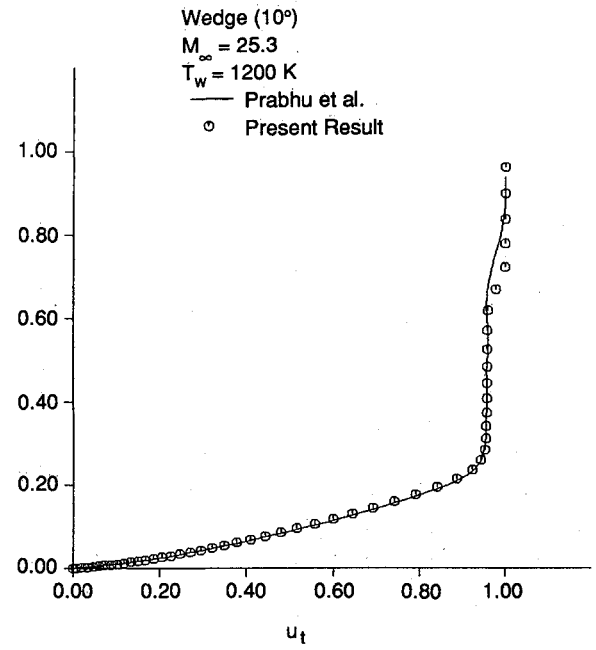

Fig. 2 Comparison of velocity profiles at $x = 1.0$.

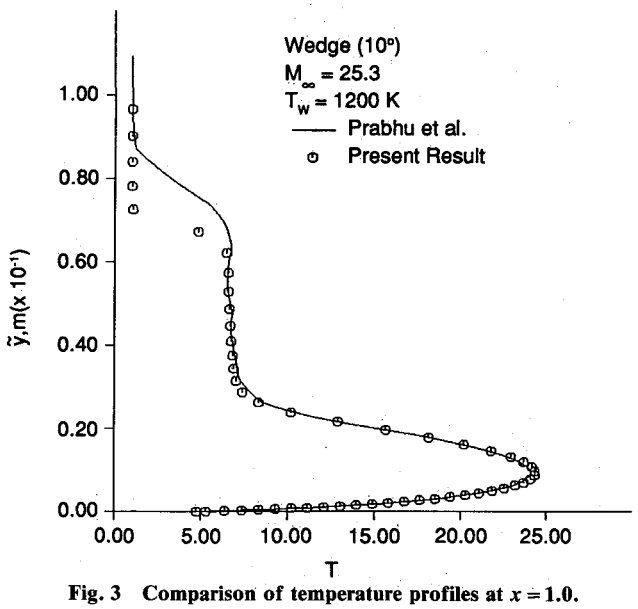

Fig. 3 Comparison of temperature profiles at $x = 1.0$.

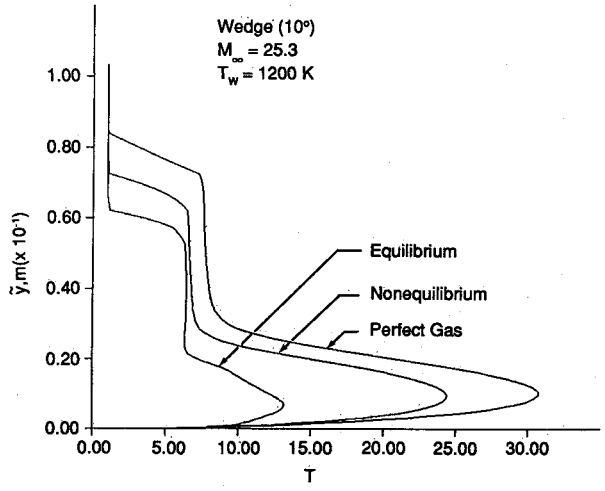

Fig. 4 Comparison of temperature profiles for perfect gas, equilibrium, and nonequilibrium chemistry.

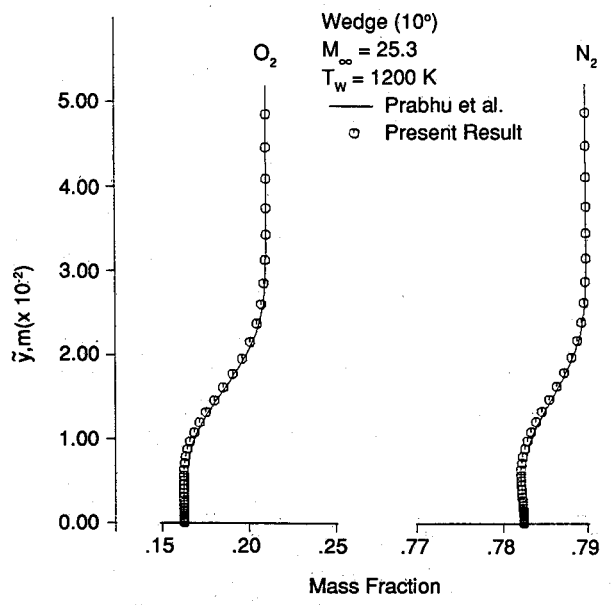

Fig. 5 Comparison of O_2 and N_2 mass fraction profiles at $x = 1.0$.

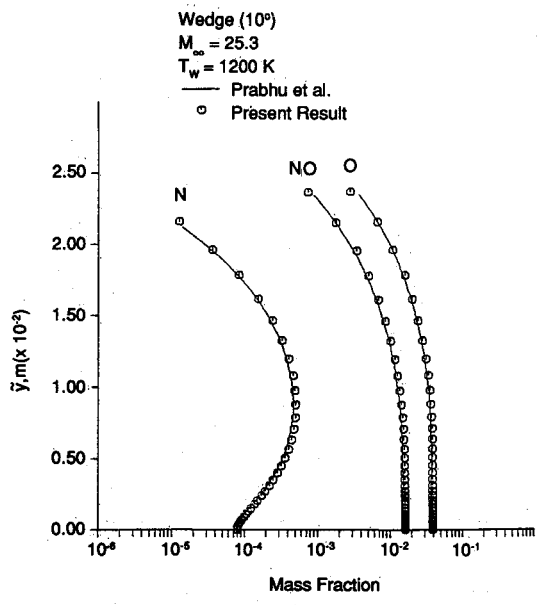

Fig. 6 Comparison of N, O, and NO mass fraction profiles at $x = 1.0$.

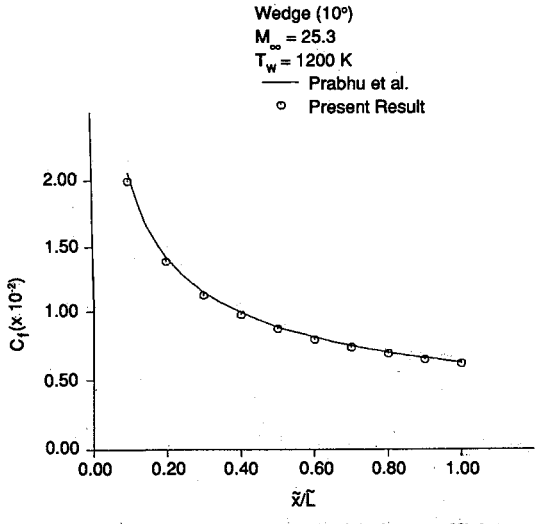

Fig. 7 Comparison of skin-friction coefficients.

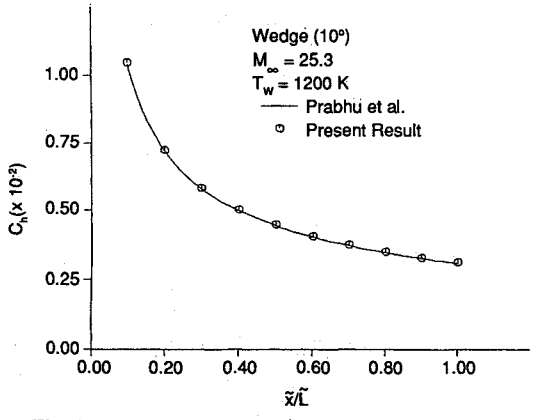

Fig. 8 Comparison of heat-transfer coefficients.

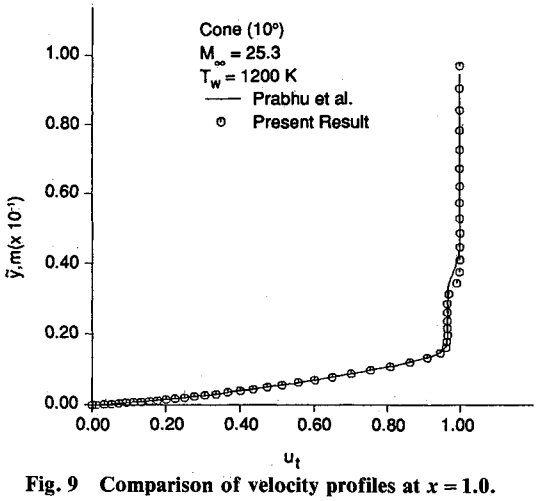

Fig. 9 Comparison of velocity profiles at $x = 1.0$.

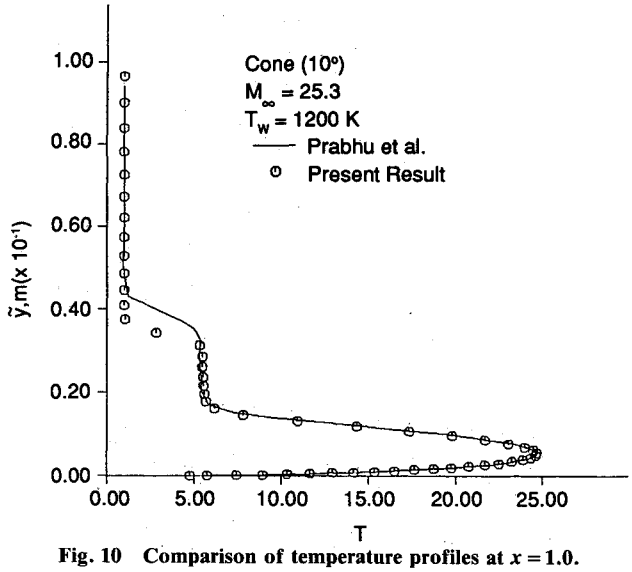

Fig. 10 Comparison of temperature profiles at $x = 1.0$.

noncatalytic wall boundary condition was used. The results from the present code are in excellent agreement with the results from the fully coupled code of Prabhu et al., provided that the smoothing coefficients in the latter code are adjusted to relatively low values. The computed mass fractions were found to be quite sensitive to the values of the smoothing coefficients in the Prabhu code. On the other hand, smoothing is not necessary for the present upwind calculations.

Figures 7 and 8 display the streamwise variations of the coefficients of skin friction and heat transfer. The formulas used to compute these quantities are

$$C_f = \frac{2\mu_w}{Re_\infty}\frac{\partial u}{\partial n} \tag{19}$$

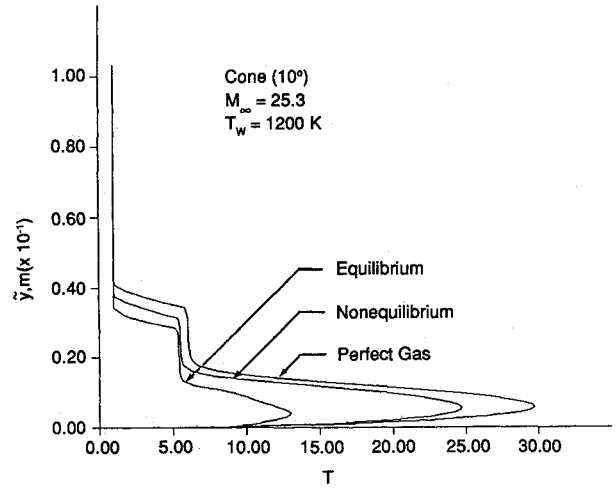

Fig. 11 Comparison of temperature profiles for perfect gas, equilibrium, and nonequilibrium chemistry.

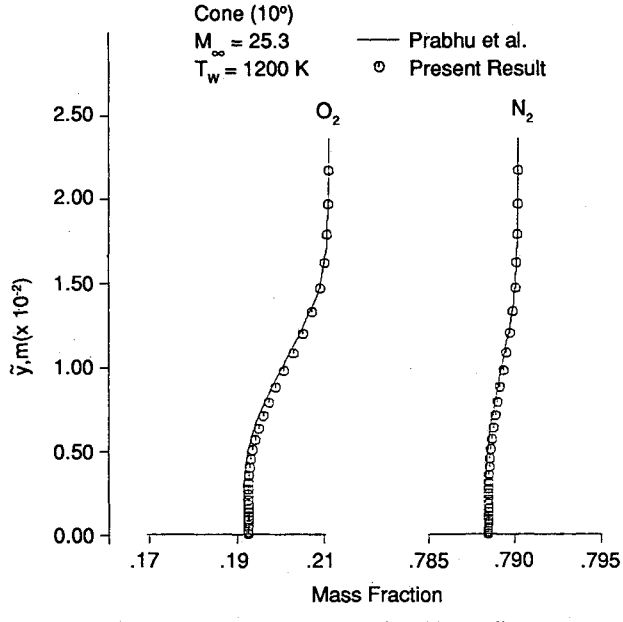

Fig. 12 Comparison of O_2 and N_2 mass fraction profiles at $x = 1.0$.

$$C_h = \frac{\mu_w}{Pr_\infty Re_\infty}\frac{1}{\left[\dfrac{(\gamma_\infty - 1)M_\infty^2}{2} + 1 - T_w\right]}\frac{\partial T}{\partial n} \tag{20}$$

where n represents the distance normal to the wall. The heat-transfer coefficient reflects only the conductive heating rate. The diffusive heating rate was negligible for this problem. The agreement between the two codes is excellent for these coefficients.

Test Case II

The second test case computed was that of hypersonic, laminar flow of chemically reacting air over a 10-deg half-angle cone. This case provides a test for the axisymmetric capability of the code. The initial conditions, step size, and grid for this problem are identical to those used for the wedge in test case I.

The tangential velocity and temperature profiles at $\tilde{x} = 1.0$ m are compared in Figs. 9 and 10. The results agree very well, except in the vicinity of the shock wave, where the smoothing in the centrally differenced code "smears" the solution. The nonequilibrium, equilibrium, and perfect gas ($\gamma_\infty = 1.4$) tem

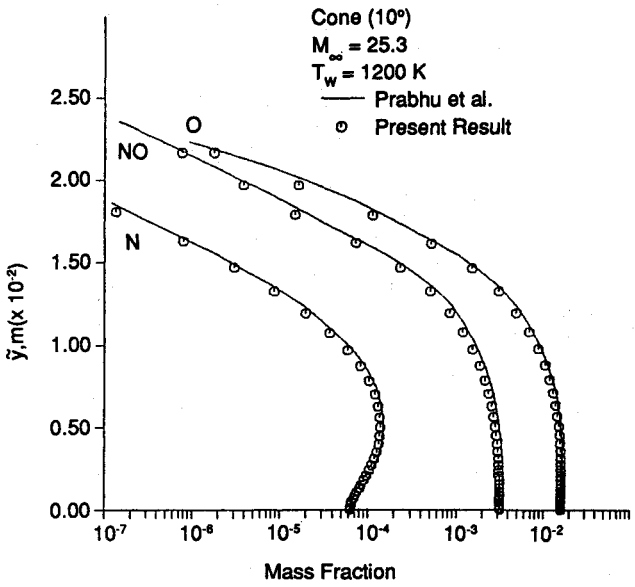

Fig. 13 Comparison of N, O, and NO mass fraction profiles at $x = 1.0$.

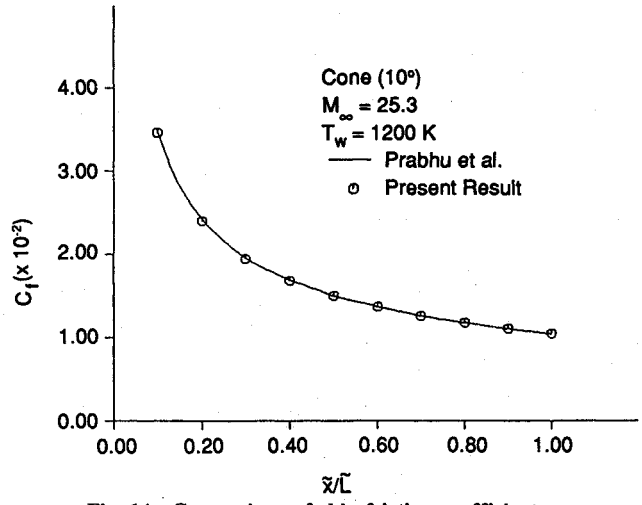

Fig. 14 Comparison of skin-friction coefficients.

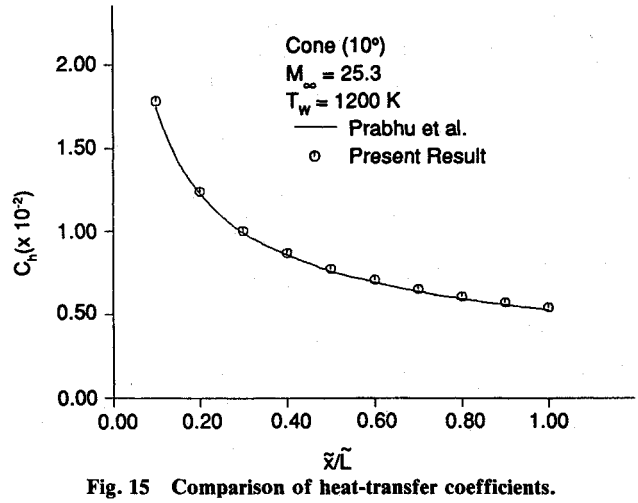

Fig. 15 Comparison of heat-transfer coefficients.

perature profiles (computed with the present upwind code) are shown in Fig. 11. The mass fractions of O_2, O, N_2, N, and NO at $\tilde{x} = 1.0$ m are compared in Figs. 12 and 13. The results from the present loosely coupled code are in excellent agreement with the results from the fully coupled code of Prabhu et al. The streamwise distributions of the skin friction and heat transfer coefficients are compared in Figs. 14 and 15 and show excellent agreement.

All of the computations were performed on an Apollo DN3000 workstation. An indication of the relative computer effort required by the two PNS codes to compute the chemically reacting flowfields is given by a comparison of the CPU times. To compute the present test cases, the fully coupled, central-difference code of Prabhu et al. required 0.080 s per step per grid point, whereas the present loosely coupled upwind code required 0.054 s per step per grid point. The present upwind code takes approximately the same amount of computer time to compute a nonequilibrium case as it does to compute an equilibrium case, provided the solution is not recomputed at the $n+1$ station.

Concluding Remarks

A new, real gas, upwind, PNS code has been developed to compute two-dimensional/axisymmetric hypersonic flows of equilibrium or nonequilibrium chemically reacting air. The code has been used to successfully compute the $M_\infty = 25$ laminar flow of dissociating air over a wedge and cone. The results of these computations are in excellent agreement with those obtained using a centrally differenced, fully coupled, nonequilibrium PNS code, except in the vicinity of the shock wave, where the present code is clearly superior in resolving the discontinuity. The present upwind nonequilibrium PNS code is currently being extended to permit three-dimensional computations.

Acknowledgments

This work was supported by NASA Ames Research Center through Small Business Innovation Research (SBIR) Contract NAS2-12552 and by the Engineering Research Institute, Iowa State University. The Technical Monitor for this contract was Dr. Terry L. Holst.

References

[1]Li, C. P., "Numerical Simulation of Re-entry Flow Around the Space Shuttle Orbiter Including Real Gas Effects," *Computers in Flow Predictions and Fluid Dynamics Experiments,* American Society of Mechanical Engineers, Nov. 1981, pp. 141–149.

[2]Gnoffo, P. A., "Hypersonic Flows Over Biconics Using a Variable-Effective-Gamma Parabolized Navier-Stokes Code," AIAA Paper 83-1666, July 1983.

[3]Prabhu, D. K. and Tannehill, J. C., "Numerical Solution of Space Shuttle Orbiter Flow Field Including Real Gas Effects," AIAA Paper 84-1747, June 1984; also *Journal of Spacecraft and Rockets,* Vol. 23, No. 3, May–June 1986, pp. 264–272.

[4]Bhutta, B. A., Lewis, C. H., and Kautz, F. A., II, "Hypersonic Equilibrium—Air Flows Using an Implicit Non-Iterative Parabolized Navier-Stokes Scheme," AIAA Paper 85-0169, Jan. 1985.

[5]Banken, G. J., Roberts, D. W., Holcomb, J. E., and Birch, S. R., "An Investigation of Film Cooling on a Hypersonic Vehicle Using a PNS Flow Analysis Code," AIAA Paper 85-1591, July 1985.

[6]Molvik, G. A., "A Parabolized Navier-Stokes Code with Real Gas Effects," presented at the 1985 Parabolized Navier-Stokes Code Workshop, Wright-Patterson AFB, OH, Sept. 1985.

[7]Stalnaker, J. F., Nicholson, L. A., Hauline, D. S., and McGraw, E. H., "Improvements to the AFWAL PNS Code Formulation," Air Force Wright Aeronautical Laboratories TR86-3076, Sept. 1976.

[8]Bhutta, B. A., Lewis, C. H., and Kautz, F. A., II, "A Fast Fully-Iterative Parabolized Navier-Stokes Scheme for Chemically-Reacting Reentry Flows," AIAA Paper 85-0926, June 1985.

[9]Sinha, N. and Dash, S. M., "Parabolized Navier-Stokes Analysis of Ducted Turbulent Mixing Problems with Finite-Rate Chemistry," AIAA Paper 86-0004, Jan. 1986.

[10]Prabhu, D. K., Tannehill, J. C., and Marvin, J. G., "A New PNS Code for Chemical Nonequilibrium Flows," AIAA Paper 87-0248, Jan. 1987.

[11]Prabhu, D. K., Tannehill, J. C., and Marvin, J. G., "A New PNS Code for Three-Dimensional Chemically Reacting Flows," AIAA Paper 87-1472, June 1987.

[12]Sinha, N., Dash, S. M., and Krawczyk, W. J., "Inclusion of Chemical Kinetics into Beam-Warming Based PNS Model for Hypersonic Propulsion Applications," AIAA Paper 87-1898, June-July 1987.

[13]Gielda, T. P., Hunter, L. G., and Chawner, J. R., "Efficient Parabolized Navier-Stokes Solutions of Three-Dimensional, Chemically Reacting Scramjet Flowfields," AIAA Paper 88-0096, Jan. 1988.

[14]Chitsomboon, T. and Northam, G. B., "A 3D-PNS Computer Code for the Calculation of Supersonic Combusting Flows," AIAA Paper 88-0438, Jan. 1988.

[15]Beam, R. and Warming, R. F., "An Implicit Factored Scheme for the Compressible Navier-Stokes Equations," *AIAA Journal,* Vol. 16, April 1978, pp. 393-401.

[16]Lawrence, S. L., Tannehill, J. C., and Chaussee, D. S., "An Upwind Algorithm for the Parabolized Navier-Stokes Equations," AIAA Paper 86-1117, May 1986.

[17]Lawrence, S. L., Chaussee, D. S., and Tannehill, J. C., "Application of an Upwind Algorithm to the Three-Dimensional Parabolized Navier-Stokes Equations," AIAA Paper 87-1112, June 1987.

[18]Roe, P. L., "Approximate Riemann Solvers, Parameters, Vectors, and Difference Schemes," *Journal of Computational Physics,* Vol. 43, No. 2, 1983, pp. 357-372.

[19]Tannehill, J. C., Ievalts, J. O., and Lawrence, S. L., "An Upwind Parabolized Navier-Stokes Code for Real Gas Flows," AIAA Paper 88-0713, Jan. 1988.

[20]Balakrishnan, A., "Application of a Flux-Split Algorithm to Chemically Relaxing, Hypervelocity Blunt Body Flows," AIAA Paper 87-1578, June 1987.

[21]Srinivasan, S., Tannehill, J. C., and Weilmuenster, K. J., "Simplified Curve Fits for the Thermodynamic Properties of Equilibrium Air," NASA RP-1181, Aug. 1987.

[22]Srinivasan, S., Tannehill, J. C., and Weilmuenster, K. J., "Simplified Curve Fits for the Transport Properties of Equilibrium Air," NASA CR-178411, Dec. 1987.

[23]Vigneron, Y. C., Rakich, J. V., and Tannehill, J. C., "Calculation of Supersonic Viscous Flow Over Delta Wings with Sharp Subsonic Leading Edges," AIAA Paper 78-1137, July 1978.

[24]Tannehill, J. C., Ievalts, J. O., Prabhu, D. K., and Lawrence, S. L., "An Upwind Parabolized Navier-Stokes Code for Chemically Reacting Flows," AIAA Paper 88-2614, June 1988.

[25]Blottner, F. G., Johnson, M., and Ellis, M., "Chemically Reacting Viscous Flow Program for Multi-Component Gas Mixtures," Sandia Labs., Albuquerque, NM, Rept. SC-RR-70-754, Dec. 1971.

[26]Wilke, C. R., "A Viscosity Equation for Gas Mixtures," *Journal of Chemical Physics,* Vol. 18, No. 4, April 1950, p. 517.

[27]Grossman, B. and Walters, R. W., "An Analysis of Flux-Split Algorithms for Euler's Equations with Real Gases," AIAA Paper 87-1117-CP, June 1987.

[28]Colella, P. and Glaz, P. M., "Efficient Solution Algorithms for the Riemann Problem for Real Gases," *Journal of Computational Physics,* Vol. 59, 1985, pp. 264-289.

[29]Anderson, D. A., Tannehill, J. C., and Pletcher, R. H., *Computational Fluid Mechanics and Heat Transfer,* Hemisphere, New York, 1984.